

Design and Analysis of Enhancing Impedance Bandwidth and high Isolation Characteristics of UWB MIMO Antennas

Shivanand Konade, Manoj Dongre

Submitted: 25/01/2024 Revised: 03/03/2024 Accepted: 11/03/2024

Abstract-A small dual band-notched two port multiple input and multiple output antenna with low mutual coupling for ultra-wide band systems is the subject of this planned research study. The two identical monopole elements are fed by two 50Ω coplanar waveguide lines, making the total antenna dimensions of 18 X 29.5 X 1.6 mm³. Manufactured side by side on the upper surface of FR-4 ground plane substrates. A T-shaped stub was substituted for the rectangular stub in order to lessen the mutual coupling between the parts. The suggested antenna covers the UWB spectrum and records a wide resistance bandwidth at each port between 2.3 and 12GHz. This antenna has a modest size and design. The element's mutual coupling is less than -20 dB. Efficiency is 85% and the envelope correlation coefficient is less than 0.04. Evaluation of antenna parameters is done in terms of return loss, gain, DC, and ECC.

Keywords: Compact, MIMO, band notch characteristics for mutual coupling, and UWB antenna

1. Introduction

The authorized and unlicensed frequency range of 3.1 to 10.6 GHz was assigned by the Federal Communication Commission (FCC) [1]. Since then, UWB technology has been developed, providing a number of advantages such as low power spectra density, high precision range, and high data rate transmission. and more has attracted a lot of attention. Multiple input multiple output (MIMO) technology and UWB technology work together to solve multipath fading and boost UWB system capacity without requiring an extra frequency range. Since MIMO technology demands MIMO antennas with small mutual coupling, particularly for portable devices with limited space, many techniques are utilized to lower the overall dimensions and mutual coupling between the elements of these antennas. For example, high isolation of more than 20 dB is produced by adding two modified T-shape [5], These UWB MIMO antennas incorporate two F-shape [4], two inverted L-shape [3], and two stubs into the shared ground plane. To reduce the mutual coupling to less than -16 dB, a tree-like structure is also inserted in [6] between two UWB MIMO antenna elements. The two MIMO antenna elements are positioned perpendicular to one another in order to minimize mutual coupling as stated in [7] and [8]. In both cases, mutual coupling of less than -15 and -20 dB is obtained throughout the entire UWB spectrum.

Additionally, an electromagnetic band gap (EBG) structure has been added between the two in order to lessen the mutual coupling between [9] and [10].

elements and, via the UWB spectrum, an isolation of more than 20 and 25 dB, respectively. Subsequent integrated waveguide (SIW) constructions have been employed in [11–13] to decrease the mutual coupling of a 34 × 34 array antenna, a 4-element antenna, and a 2-element antenna down to -15, -20, and -25 dB, in that order. Furthermore, to reduce the mutual coupling of the MIMO antenna's component parts to less than -20 dB, a metamaterial structure is suggested in [14]. Other methods for reducing mutual coupling include the use of radial stub loaded resonator (RSLR) or wideband neutralization line, which are studied in [15] and [16], respectively. Over the working bandwidth, an isolation of greater than 22 and 25 dB is established in each case. The interference between UWB signals has drawn a lot of attention to UWB antennas with band-notched features. range (3.1 – 10.6 GHz) and some other frequency bands, such as 3.3 – 3.7 GHz for Worldwide Interoperability for Microwave Access (WiMAX), 5.15 – 5.825 GHz for Wireless Local Area Network (WLAN), 3.7 – 4.2 GHz for C-band, and 7.7 – 8.5 GHz for X-band satellite communication. Many design configurations and techniques have been investigated to reduce these interferences. For example, in order to achieve dual band-notched features, two open ended inverted L-shaped slots are introduced on the radiating patch of a small tapered fed MIMO antenna described in [17]. Creating distinct shaped etchings on the feed-line [18], radiating patch [19], or ground plane Other examples of these techniques to obtain UWB antennas with single or multiple band-notched characteristics include placing different strips near the feed-line [23] or near the ground plane [24], and using parasitic elements like bended dual L-shaped branches [25] and an open ended F-shape stub

Electronics and Telecommunication Department Ramrao Adik Institution of Technology, Dr. D. Y. Patil University, Nerul, Navi Mumbai
E-mail: shivanand.konade@dypatil.edu, manoj.dongre@dypatil.edu

[26]. Additionally, [27] demonstrates a compact, triple band notched UWB MIMO antenna with two circular split rings of the single slot kind of $30 \times 60 \times 1 \text{ mm}^3$ with a wide impedance bandwidth of roughly 118%. two C-shaped strips next to the feed line and a resonator in the radiator, respectively, to lessen interference from X-band, WLAN, and WiMAX. An MIMO dual band-notched UWB antenna measuring $26 \times 26 \times 0.76 \text{ mm}^3$ is displayed in [28]. To filter WLAN and X-band interference, four rectangular strips are printed near the feed line. , and a T-shaped groove is etched out of the ground plane to lessen mutual coupling between elements. Based on a basic dual band-notched UWB MIMO antenna with low mutual coupling ($|S_{12}|$ less than -20 dB) and a tiny dimension of $18 \times 35 \times 1.6 \text{ mm}^3$, the designed and simulated technique is relatively compact in comparison to most earlier works [29]. With a total size of $18 \times 18 \times 1.6 \text{ mm}^3$, The two monopoles that make up the suggested antenna are identical. A tiny single input single output (SISO) is what each monopole is dual band-notched UWB antenna that is supplied by a 50Ω coplanar waveguide. The suggested MIMO antenna is achieved by aligning two elements next to one another and inserting a T-shaped stub into the shared ground plane between them. A T-shaped stub that has been etched with a long, vertical, rectangular slot results in isolation that is greater than 20 dB over the whole frequency range. This technique also allows us to create a very small and compact antenna with a wide impedance bandwidth for both ports from 2.3 to 12 GHz of about 135% ($|S_{11}|$ less than -10dB). Subsequently, using the built-in two-port MIMO antenna, a four element UWB antenna measuring $35 \times 37 \times 1.6 \text{ mm}^3$ is provided, and the S-parameters are examined. To produce notch bands around the WiMAX and WLAN bands, two half-wavelength rectangular single complementary split-ring resonators (RSCSRRs) of different lengths were etched out of the radiating patch. This antenna provides nearly omnidirectional radiation pattern, high radiation efficiency, acceptable gain, and a minimal envelope correlation coefficient (ECC) of about 0.04. It is also incredibly small in size. Its isolation between two ports is likewise very great. An FR-4 substrate was used to build the recommended antenna, and it was examined experimentally. Following the presentation and discussion of the measured results, a good agreement between the simulated and measured outcomes was observed.

2. Design Of Antennas

2.1. Design of RSCSRRs and Antenna Configuration

The MIMO antenna's construction on a $18 \times 29.5 \times 1.6 \text{ mm}^2$ substrate is illustrated in Figure 1. The planned antenna is built on a FR4 substrate with a dielectric

constant of $\epsilon_r = 4.4$ and a loss tangent of 0.02. The antenna is made up of two right triangle radiating elements connected by a 50Ω microstrip line.

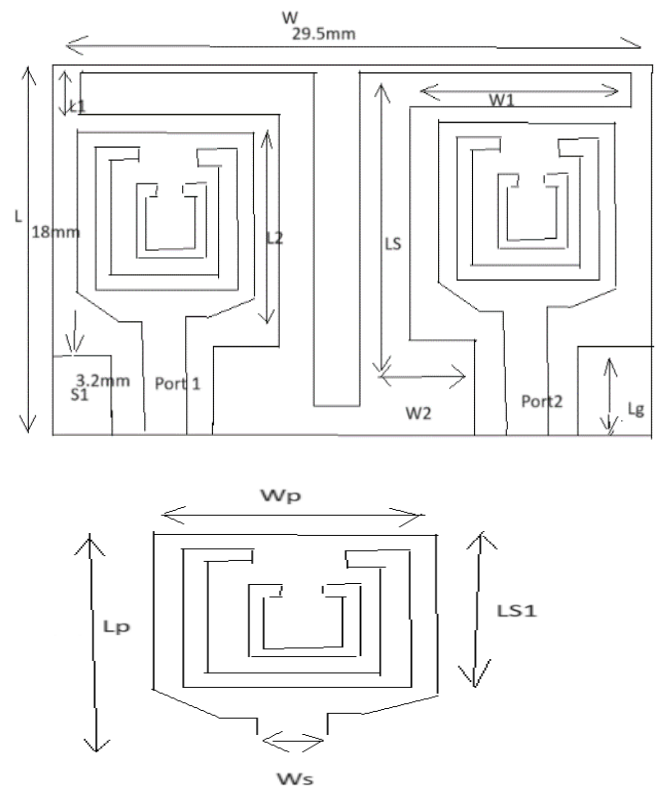


Fig 1(a). The figure structure of the planned antenna
Figure 1(b) shows the placement and geometry of RSCSRRs inside the radiating region.

The MIMO antenna's final optimization was performed at a reasonable cost for FR4 substrate. Its dimensions are $18 \times 29.5 \times 1.6 \text{ mm}^2$ with a dielectric constant.

$\epsilon_r = 4.4$ and thickness is $h=1.6\text{mm}$ to achieve 50Ω impedance for the mutual coupling between the two port and T-shaped stub to shared rectangular and ground plane between the two elements. The interference of WLAN from 5.15 to 5.825GHz and WiMAX from 3.3 to 3.7GHz.

The correct length of two slots can be obtain for the filter mentioned band following design equation. $L_n = 2x(W_{sn} + L_{sn}) - (g_n)$

$$L_n = \frac{c}{2f_{\text{Notch}}\sqrt{\epsilon_{\text{eff}}}} = \frac{\lambda_g}{2} \quad (1)$$

The WiMAX band rejection is obtained for the WLAN band filter and for $n=2$ The length and width of RSCSRRs and the defined small gap are denoted by L_{sn} and W_{sn} is the length and width of RSCSRRs and small gap defined as g_n . C is the speed of light, and f_{Notch} is the central frequency for the notched and ϵ_{eff} for the effective

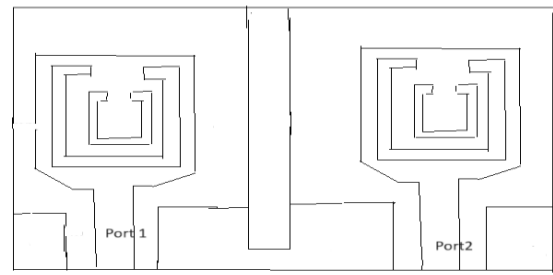
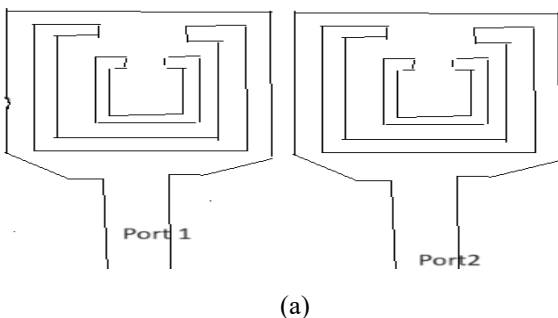
dielectric constant of the substrate that can be obtain for the following equation

$$\epsilon_{eff} = \frac{\epsilon r + 1}{2} + \frac{\epsilon r - 1}{2} \left(1 + \frac{12h}{w_f}\right)^{-\frac{1}{2}} \quad (2)$$

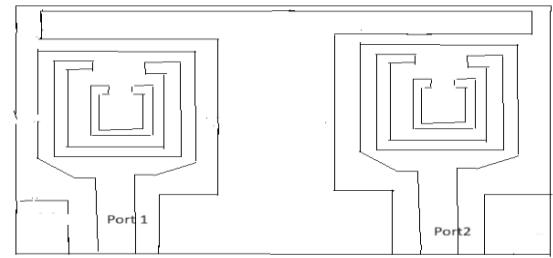
Wherever w_f is the substrate's thickness, and h is the feed line's width.. When f_{Notch} for the ideal proportions of S_1 and S_2 for the WLAN is 5.3GHz and WiMAX is 3.4GHz respectively.

2.2 The Process of Antenna Design

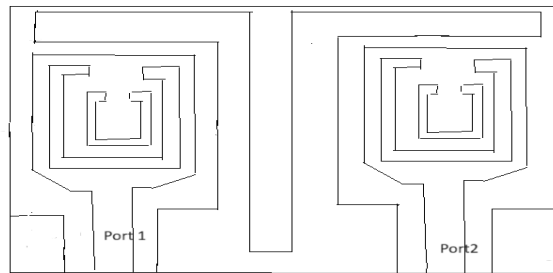
Four distinct T-shaped ground stubs are utilized to identify the radiator of the RSCSRRs, which has a rectangular cut on it. Figures 2(a) through (b) depict the process of creating the final MIMO antenna parameters for each evolutionary design stage in the model. Figure 2(a) displays the two matching CPW-fed for the antenna of the elements that are still positioned at a length of $d=11$ mm. The resistance antenna bandwidth, which is about 7 GHz from 5 to 12 GHz for each port, is shown in Figure 3. The first stage is displayed in Figure 3. They can't cover the UWB spectrum as a result, and the operating bandwidth provides very little isolation. The vertical rectangular stub of the second antenna is at the center. For $(|S_{12}|)$, the antenna exhibits mutual coupling. Consequently, by outweighing the interferences from WLAN and WiMAX separately, the mutual coupling lessens. The impacts of the vertical cut at lesser frequencies are being felt. This has an isolation of less than -20dB throughout the whole operational bandwidth and spans from 2.3 to 12GHz at the twin notch bands. Equations (1) and (2) provide the ideal positions for them. WiMAX interferences peak at 3.7GHz with VSWR=113 and extend from 3.1GHz to 4.8GHz in frequency. lower RSCSRR consumption The total length is 16 mm, providing additional frequency notch band for filtering. About 1.2 GHz is covered by the 5.1 to 6.3 GHz WLAN band, with combined ports at 5.3 GHz having the greatest VSWR of 31. Table 1 displays the final, presumed optimal dimension. The earth's plane is shifting. It not only improves the antenna's impedance matching at 53% but also lowers the mutual coupling to less than -20dB. The ground T-shaped stub is positioned to provide impedance matching.



(b)



(c)



(d)

Fig 2. Four design antenna repetitions

With the exception of the two notch bands mostly affects lower frequencies and enhances impedance matching; as a result, the vertical cut produces an isolation of less than -20 dB over the whole operating spectrum and a relative impedance bandwidth of 135% from 2.3 to 12 GHz. Equations (1) and (2) can be used to calculate the proper size of the two RSCSRRs. and their locations have been optimized. The second frequency notch band to filter the WLAN spectrum from 5.1 to 6.3 GHz, encompassing roughly 1.2 GHz, with peak VSWR=113 at 3.7 GHz, is provided by the smaller RSCSRR, which has a total length of 17 mm. With a total length of 25.2 mm, the bigger RSCSRR lessens WiMAX spectrum interference from 3.1 to 4.8 GHz, which covers 1.7 GHz.

Table 1. Optimized values for dimensions of UWB MIMO antenna.

Parameters	Dimensions (mm)	Parameters	Dimensions (mm)
L	18	XF	3
W	29.5	SL	11

L1	9.1	SW	4.5
W1	4.9	SW1	2
L2	3.6	SL1	1
W2	4.9	SL2	1
G	4.47	SL3	1

ANALYSIS BAND NOTCHED

Plotting and analysis are done to determine how the dimensions of the RSCSRRs affect the notched performance and impedance bandwidth for different W_s1 and W_s2 sizes. The core frequency of WLAN rises from 4.9GHz to 5.6GHz, while the central frequency of WiMAX climbs from 3.4GHz to 4.2GHz. Both the high and center frequencies of the WLAN frequency band remain fixed. While port 2 is equivalent to a 6GHz and 50Ω load, port 1's current distribution is depicted in Figure 3. In Figure 5, the surface current is greater than the WiMAX notched band.

3. Simulated and Results

A dual band-notched MIMO antenna validates the accuracy of the simulated results. It is installed on a FR4 substrate and gauges the created object's overall form.

The extraordinarily good agreement measurements and simulated findings are shown in Figure 5. It is possible to operate the antenna in the impedance band width. The band width for 2.3 to 12 GHz is wider than that of 9 GHz. For the mutual coupling of the antenna, which is less than -20 dB, WiMAX and WLAN employ the two notched bands at (|S11|, |S22| < -10 dB). (S12, S21) < -20 dB In Figure 6. The frequencies of the two sharp decreases at the antenna's notches, which give it its signal rejection capability. This measure is significant since it illustrates the antenna element's diversity performance.

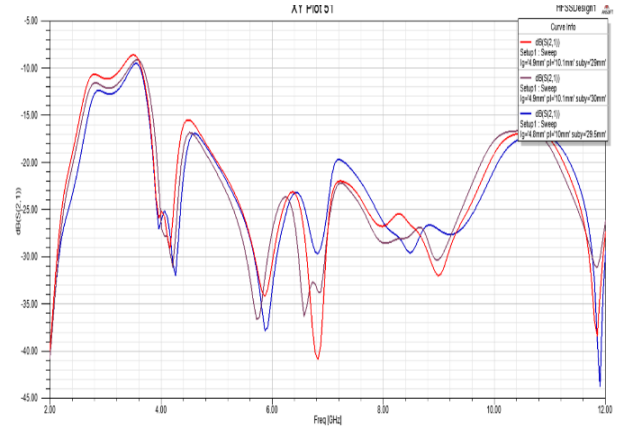
$$ECC = \frac{|S_{11}^* S_{12} + S_{21}^* S_{22}|}{(1 - |S_{11}|^2 - |S_{21}|^2)(1 - |S_{22}|^2 - |S_{12}|^2)} \quad (3)$$

Efficiency gains from two-port MIMO antennas are a crucial additional factor in defining the diversity presentation. It can be computed using the formula that follows.

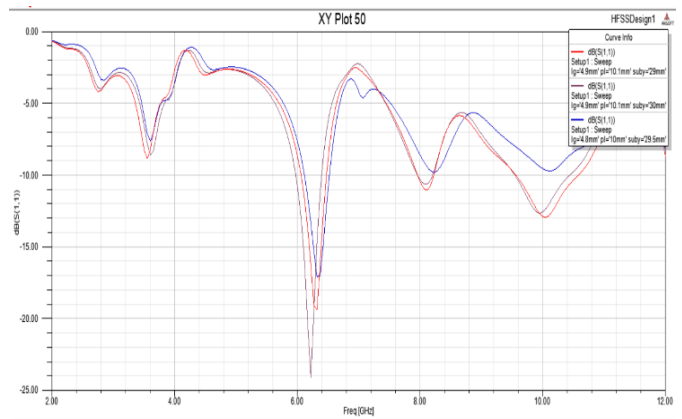
$$\eta_{max} = \sqrt{\eta_1 \eta_2} (1 - |r|^2) \quad (4)$$

Figure 7 shows the total efficiencies of ports 1 and 2, for the η_1 and η_2 , respectively, and how close they are to the ECC for the $|r|^2$ — the complex correlation magnitude between the two MIMO antenna elements squared.

For the working bandwidth, its ECC is less than 0.04. Both of its components have independent emission patterns and are designed antennas



(a)



(b)

S-parameters of the proposed antenna are shown in Figure 3. (a) |S11| and (b) |S21|.

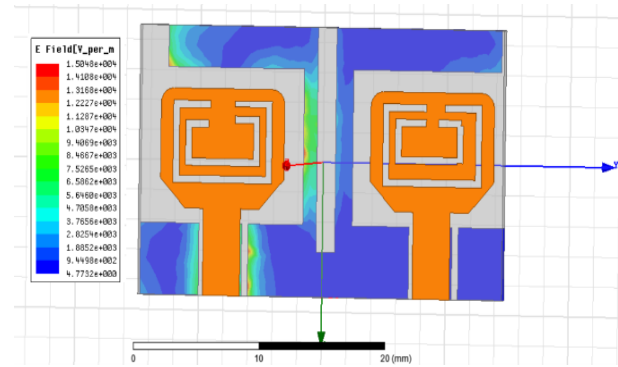
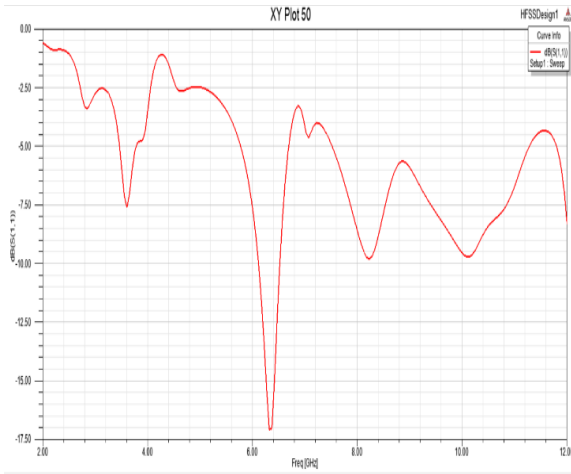
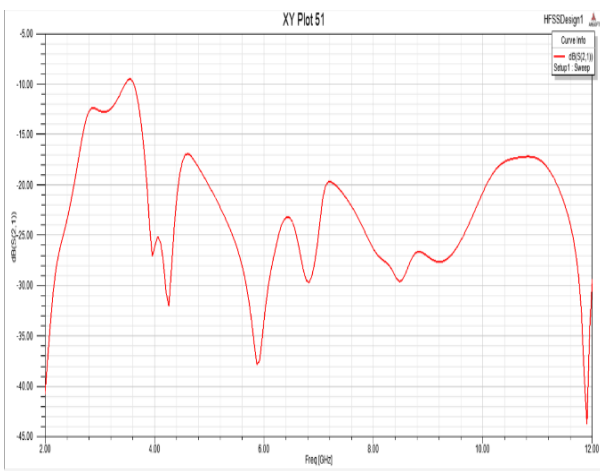


Fig 4: Distribution of the band-notched MIMO antenna's current surface at 6GHz



(a)



(b)

Fig 5. Simulated and measured S-parameters

(a) |S11| (b) |S21|.

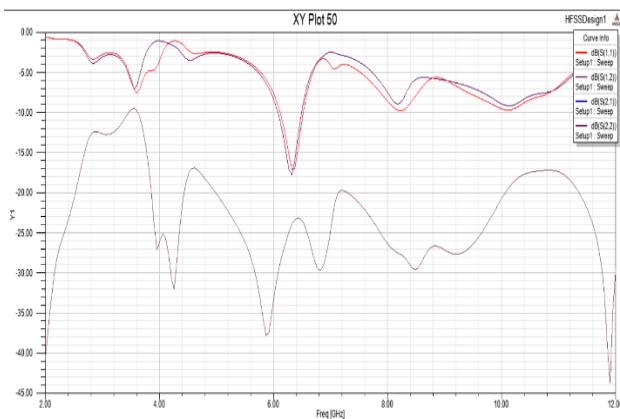


Fig 6. The four-element antenna's virtual S-parameters for element 1

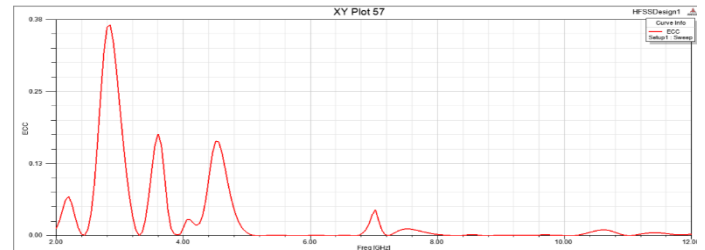


Fig 7 Efficiency and ECC versus frequency

MIMO antennas are based on two components, following the four parts of UWB. Figure 12 shows the wide resistance bandwidth, which allows WiMAX parts to function between 2.3 and 12GHz using two WLAN notched bands. Ports 1 and 2 have excellent isolation. The T-shaped stub is altered by the ground plane, and for S21, its value is less than -20dB. Space separation technique with value less than -20dB for S31 may understand ports 1 and 3. For the simulated radiation patterns, the isolation and operational bandwidth for ports 1 and 4 are less than -15dB.

Table 2. Comparison of the proposed antenna with antennas in literature.

Ref. #	Size (mm ²)	Bandwidth (GHz)	Isolation (dB)	Gain (dBi)	ECC
9	38.5 × 38.5	3.1–10.6	-15	1.4–3.6	0.02
10	40 × 80	4.5–8	-25	2–4	0.002
11	68 × 35	3.1–10.6	-20	1.7–4.2	0.002
12	40 × 20	3–11	-15	2–5	0.3
13	50 × 30	2.5–14.5	-20	0.3–4.3	0.04
14	45 × 25	3.1–12	-15	4.5	0.2
15	36 × 45	3.01–12	-20	4–8.24	0.025
16	24 × 32	3.1–12.5	-16	1–4.8	0.05
17	26 × 28	2.9–10.8	-15	1–4	0.5
18	40 × 40	3.1–11	-20	3.28	0.002
19	16 × 35	3.1–5	-22	1–4	NA
Proposed	18 × 29.5	3.1–10.6	-20	4–6	>0.04

4. Conclusions

The goal of this research is to create a rejection MIMO antenna for UWB applications with a reduced mutual coupling. The dual band with a single layer is fairly small. In total, the antenna measures 18 x 29.5 x 1.6 mm³. It covers 9.7 GHz impedance bandwidth from 2.3 GHz to 12 GHz for mutually ports-shaped stubs and has a mutual coupling of less than -20dB.

and rectangular slots onto common ground planes. In the event of a rejection, the WLAN and WiMAX bands,

which span 3.1 to 4.8GHz and 5.1 to 6.3GHz, respectively, are carved out of the RSCSRs' radiating path. In the far field, the intended antenna's omnidirectional antenna behaves well. The recommended antenna has an ECC of less than 0.04 and an efficiency of 85%. The results of the models

References

- [1] Federal Communication Commission, "First report and order in the matter of version of part of 15 of the commission's rules regarding UWB transmission systems," ET-Docket 98-153, 2002.
- [2] C. Chong, F. Watanabe and H. Inamura, "Potential of UWB Technology for the Next Generation Wireless Communications," 2006 IEEE International Symposium on Spread Spectrum Techniques and Applications, Manaus-Amazon, pp. 422-429, 2006.
- [3] M. A. Haq and S. Koziel, "Ground Plane Alterations for Design of High-Isolation Compact Wideband MIMO Antenna," IEEE Access, vol. 6, pp. 48978-48983, 2018.
- [4] Iqbal, O. A. Saraereh, A. W. Ahmad and S. Bashir, "Mutual Coupling Reduction Using F Shaped Stubs in UWB-MIMO Antenna," IEEE Access, vol. 6, pp. 2755-2759, 2018.
- [5] W. Li, Y. Hei, P. M. Grubb, X. Shi and R. T. Chen, "Compact Inkjet-Printed Flexible MIMO Antenna for UWB Applications," IEEE Access, vol. 6, pp. 50290-50298, 2018.
- [6] S. Zhang, Z. Ying, J. Xiong and S. He, "Ultra wideband MIMO/Diversity Antennas with a Tree-Like Structure to Enhance Wideband Isolation," IEEE Antennas and Wireless Propagation Letters, vol. 8, pp. 1279-1282, 2009.
- [7] S. Syedakbar, S. Ramesh and J. Deepa, "Ultra wide band monopole planar MIMO antenna for portable devices," IEEE International Conference on Electrical, Instrumentation and Communication Engineering (ICEICE), Karur, pp. 1-4, 2017.
- [8] L. Liu and T. I. Yuk, "Compact MIMO Antenna for Portable Devices in UWB Applications," IEEE Transactions on Antennas and Propagation, vol. 61, no. 8, pp. 4257-4264, 2013.
- [9] G. Saxena, P. Jain and Y. K. Awasthi, "High Isolation EBG Based MIMO Antenna for X-Band Applications," 6th International Conference on Signal Processing and Integrated Networks (SPIN), Noida, India, 2019.
- [10] T. Dabas, D. Gangwar, B. K. Kanaujia and A. K. Gautam, "Mutual coupling reduction between elements of UWB MIMO antenna using small size uniplanar EBG exhibiting multiple stop bands," International Journal of Electronics and Communications, vol. 93, pp. 32-38, 2018.
- [11] B. Niu, and J. H. Tan, "Compact four-element MIMO antenna using T-shaped and antisymmetric U-shaped slotted SIW cavities," Electronics Letters, vol. 55, no. 19, pp. 1031-1032, 2019.
- [12] B. Niu and J. H. Tan, "Compact Two-Element MIMO Antenna Based on Half-Mode SIW Cavity with High Isolation," Progress in Electromagnetics Research Letters, vol. 85, pp. 145-149, 2019.
- [13] M. Alibakhshi-kenari, B. S. Virdee, et al., "Study on isolation and radiation behaviours of a 34x34 array-antennas based on SIW and metasurface properties for applications in terahertz band over 125-300 GHz," Optik, International Journal for Light and Electron Optics, vol. 206, p. 163222, 2020.
- [14] Iqbal, O. A. Saraereh, A. Bouazizi, and A. Basir, "Metamaterial based highly isolated MIMO antenna for portable wireless communication," Electronics, vol. 7, no. 10, 2018.
- [15] S. Zhang and G. F. Pedersen, "Mutual Coupling Reduction for UWB MIMO Antennas with a Wideband Neutralization Line," IEEE Antennas and Wireless Propagation Letters, vol. 15, pp. 166-169, 2016.
- [16] Y. Li, W. Li and W. Yu, "A multi-band/UWB MIMO/diversity antenna with an enhanced isolation using radial stub loaded resonator," Applied Computational Electromagnetics Society Journal, vol. 28, no. 1, pp. 8-20, 2013.
- [17] R. Chandel, A. K. Gautam and K. Rambabu, "Tapered Fed Compact UWB MIMO-Diversity Antenna With Dual Band-Notched Characteristics," IEEE Transactions on Antennas and Propagation, vol. 66, no. 4, pp. 1677-1684, 2018.
- [18] C. R. Jetti and V. R. Nandanavanam, "Compact MIMO Antenna with WLAN Band-Notch Characteristics for Portable UWB Systems," Progress in Electromagnetics Research C, vol. 88, pp. 1-12, 2018.
- [19] M. Rahman, M. Nagshvarian Jahromi, S. S. Mirjavadi and A. M. Hamouda, "Compact UWB Band-Notched Antenna with Integrated Bluetooth for Personal Wireless Communication and UWB Applications," Electronics, vol. 8, no. 2, pp. 242-252, 2019.
- [20] M. Sharma, Y. K. Awasthi and H. Singh, "Design of CPW-Fed High Rejection Triple Band-Notch UWB Antenna on Silicon Substrate with Diverse Wireless Applications," Progress

in *Electromagnetics Research C*, vol. 74, pp. 19-30, 2017.

- [21] D. Sarkar, K. V. Srivastava and K. Saurav, "A Compact Microstrip-Fed Triple Band-Notched UWB Monopole Antenna," *IEEE Antennas and Wireless Propagation Letters*, vol. 13, pp. 396-399, 2014.
- [22] S. Lakrit, S. Das, S. Ghosh and B.T. Madhav, "Compact UWB flexible elliptical CPW-fed antenna with triple notch bands for wireless communications," *Int. J. of RF, Microwave Computational Eng.* vol.7, pp.1-14, 2020.
- [23] M. Nejati Jahromi, M. Nagshvarian Jahromi and M. Rahman, "A New Compact Planar Antenna for Switching between UWB, Narrow Band and UWB with Tunable-notch Behaviors for UWB and WLAN Applications," *Appl. Comput. Electromagn. Soc. J.*, vol. 33, pp. 400-406, 2018.
- [24] A. A. Ibrahim, M. A. Abdalla and A. Boutejdar, "A Printed Compact Band-Notched Antenna Using Octagonal Radiating Patch and Meander Slot Technique for UWB Applications," *Progress in Electromagnetics Research M*, vol. 54, pp. 153-162, 2017.
- [25] X. L. Liu, Y. Z. Yin, P. A. Liu, J. H. Wang and B. Xu, "A CPW-Fed Dual Band-Notched UWB Antenna with a Pair of Bended Dual-L-Shape Parasitic Branches," *Progress in Electromagnetics Research*, vol. 136, pp. 623-634, 2013.
- [26] J. Lee, K. Kim, H. Ryu and J. Woo, "A Compact Ultrawideband MIMO Antenna With WLAN Band-Rejected Operation for Mobile Devices," *IEEE Antennas and Wireless Propagation Letters*, vol. 11, pp. 990-993, 2012.
- [27] H. H. Liu, Y. Zhang and S. S. Gong, "Compact polarization diversity ultrawideband MIMO antenna with triple band-notched characteristics," *Microw. Opt. Technol. Lett.*, vol.57(4), pp. 946-953, 2015.
- [28] Z. Li, C. Yin and X. Zhu, "Compact UWB MIMO Vivaldi Antenna With Dual Band-Notched Characteristics," *IEEE Access*, vol. 7, pp. 38696-38701, 2019.
- [29] S. Blanch and I. Corbella, "Exact representation of antenna system diversity performance from input parameter description," *Electronics Letters*, vol. 39, no. 9, pp. 705-707, 2003.
- [30] R. Tian, B. K. Lau and Z. Ying, "Multiplexing efficiency of MIMO antennas," *IEEE Antennas and Wireless Propagation Letters*, vol. 10, pp. 183-186, 2011.